Journal of Fusion Energy, Vol. 25, No. 3/4, December 2006 (© 2006)
DOI: 10.1007/s10894-006-9014-9

Thermodynamic's Second Law Analysis for Laminar Non-Newtonian Fluid Flow

H. G. Langeroudi* **and C. Aghanajafi**

In this paper, the entropy generation of a non-Newtonian fluid such as Tho_2 inside a circular channel with constant surface temperature has been investigated. The pressure gradient along the pipe line, the difference between the dimensionless inlet wall temperature and fluid temperature and modified Stanton number are the key elements to calculate the entropy generation for three different non-Newtonian fluids. Also the variation of the dimensionless entropy generation and the pumping power to heat transfer rate ratio is calculated for two different cases, the first case involves fixed pipe length and variable inlet temperature and the second case considers fixed fluid inlet temperature and variable pipe length.

KEY WORDS: Non-Newtonian fluid; dimensionless entropy generation; pressure gradient; pumping power.

NOMENCLATURE

C_p:	specific heat capacity (J/kg K)
R:	pipe radius (m)
Ec:	Eckert number [$\bar{U}^2/[C_p(T_w - T_0)]$]
f:	friction factor
$\bar{h}$:	average heat transfer coefficient (W/m^2 K)
$\bar{h}_{c.p}$:	constant property average heat transfer coefficient (W/m^2 K)
k:	thermal conductivity (W/m K)
l:	length of the pipe (m)
$\dot{m}$:	mass flow rate (kg/s)
P:	pressure (N/m^2)
τ_0:	yield
μ_0:	viscosity yield shear stress (N/m^2)
τ_R:	shear stress in R radius (N s/m^2)
T_0:	inlet fluid temperature (K)
R_p:	ratio of the plug radius to pipe radius = (r_p/R)
Q:	flow flux m^3/s
Re:	Reynolds number $[\rho\bar{U}D/\mu]$
s:	entropy (J/kg K)
$\dot{S}_{gen}$:	entropy generation (W/K)
St:	Stanton number $[\bar{h}/(\rho\bar{U}(C_p)]$
T:	temperature (K)
T_{ref}:	reference temperature (=293 K)
T_w:	wall temperature the pipe (K)
$\bar{U}$:	fluid bulk velocity (m/s)
P_r:	pumping power to heat transfer rate ratio
Ψ:	dimensionless entropy generation $[\dot{S}_{gen}/[\dot{Q}/(T_w - T_0)]$
D:	Pipe diameter (m)
λ:	dimensionless axial distance $[l/D]$
Π_1:	modified Stanton number $[St\ \lambda]$
Π_2:	dimensionless group $[Ec/(St\ Re)]$
ρ:	density (kg/m^3)
τ:	dimensionless inlet wall-to-fluid
μ_b:	viscosity of fluid at bulk temperature (N s/ m^2)
x:	axial distance (m)
ΔT:	increase of fluid temperature (K)
μ:	viscosity (N s/ m^2)
r_0:	plug radius for Bingham fluid (m)
r_p:	plug radius for Casson model (m)
V_z:	velocity along the pipe for Bingham model (m/s)
n:	the degree of non-Newtonian fluid for power-law model

Department of Mechanical Engineering, K.N.T. University of Technology, Tehran, Iran.
*To whom correspondence should be addressed. E-mail: hossein_ghalyanchi@yahoo.com

INTRODUCTION

The entropy generation plays an important role in the design and development of thermo-fluid components. The optimal design of these components can be achieved by minimizing the entropy generation.

Entropy generation is increased by the presence of high gradients in velocity and temperature in the development of know-how for the heat exchanger industry. We strive for important thermal contact (enhanced-heat transfer) and reduced pump power loss in order to improve the thermodynamic efficiency of the heat exchanger. Good heat exchanger design means, ultimately, efficient thermodynamic performance, that is the least generation of entropy or least destruction of useful work in an engineering system is directly proportional to the rate of entropy generation [11].

Several modern material and manufacturing processes involve non-Newtonian fluids, and in particular viscoplastic fluids. Examples of non-Newtonian behavior can be found in processes for manufacturing coated sheets, optical fibers, foods, drilling muds and plastic polymers.

Entropy generation and minimization were investigated extensively by Bejan [1]. He showed the fundamental importance of the entropy minimization for efficient Processing. The second law analysis of combined heat and mass transfer in internal and an external flow was considered by Carrington and Sun [5]. They introduced the entropy Correlation, which could be used for internal and external flows. Heat transfer and entropy generation for a transparent gas flow were considered by Gbadebo et al. [6].

FLUID FLOW ANALYSIS IN A PIPE

Consider a constant cross-sectional area pipe shown in Figure 1. The surface temperature of the pipe is kept constant at T_w. An incompressible viscous fluid with mass flow rate, $\dot{m}$ and inlet temperature, T_0 enters the pipe of length l. Heat transfer to the bulk fluid occurs through the average heat transfer coefficient, $\bar{h}$ which is not constant but is a function of the viscosity variation. On the other hand, density ρ, thermal conductivity k, and specific heat C_p of the fluid are assumed to be constant within the range of temperatures considered. We also would like to analyze the entropy generation for several non-Newtonian fluid with different inlet temperature and length for constant viscosity.

The heat transfer rate to the fluid inside the control volume shown in Figure 1 is

$$\delta\dot{Q} = \dot{m}C_p\,dT = \bar{h}\pi D(T_w - T)\,dx, \qquad (1)$$

where $\dot{m}$ is the mass flow rate given by

$$\dot{m} = \rho\bar{U}\frac{\pi D^2}{4}$$

It should be noted that in equation (1) the pipe is assumed to have a circular cross section; however, the analysis is not affected, assuming cross-sectional areas other than circular. Integrating equation (1). The bulk temperature variation of the fluid along the pipe can be obtained as

$$T = T_w - (T_w - T_0)\exp\left(-\frac{4\bar{h}}{\rho\bar{U}DC_p}x\right) \qquad (2)$$

PRESSURE GRADIENT FOR NON-NEWTONIAN FLUIDS

According to Newton's Law of viscosity a plot of shear stress versus rate of strain for a given fluid should give a straight line through the origin, and the slope of this line is the viscosity of the fluid at the given temperature and pressure (Figure 2).

The subject of non-Newtonian flow is actually a subdivision of the larger science of rheology, this is the "science of deformation and flow" and includes the study of the mechanical properties of gases, liquids, plastics, asphalts, and crystalline materials. Numerous empirical equations, or models have been proposed to express the steady-state relation between shear stress and rate of strain. Three representative models are summarized below.

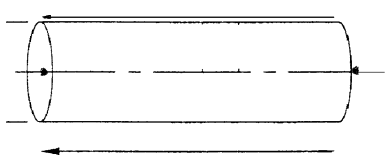

Fig. 1. Schematic view of a pipe.

Power-Law

The ostwald-de waele model is defined as:

$$\tau_{yx} = -m\left|\frac{dv_x}{dy}\right|^{n-1}\frac{dv_x}{dy} \tag{3}$$

For $n = 1$, it reduces to Newton's law of viscosity with $m = \mu$; thus the deviation of n from unity indicates the degree of deviation from Newtonian behavior. Approximate values of m and n for various fluids are given in [12].

The velocity profile using power-law model is obtained by the shell method and is represented by

$$u = \frac{n}{n+1}\left(-\frac{1}{2\mu}\left(\frac{\partial p}{\partial x}\right)\right)^{\frac{1}{n}}\left(R^{\frac{1}{n}+1} - r^{\frac{1}{n}+1}\right) \tag{4}$$

The volume flow rate, the average velocity and the pressure gradient are represented by the equations (5–7):

$$Q = \int_0^R u(2\pi r)\,dr$$

$$Q = \frac{2\pi n}{(n+1)}\left(-\frac{1}{2\mu}\left(\frac{\partial p}{\partial x}\right)\right)^{\frac{1}{n}}\left(\frac{R^{\frac{3n+1}{n}}}{2} - \frac{n}{3n+1}R^{\frac{3n+1}{n}}\right) \tag{5}$$

$$\overline{U} = \frac{2n}{R^2(n+1)}\left(-\frac{1}{2\mu}\left(\frac{\partial p}{\partial x}\right)\right)^{\frac{1}{n}}\left(\frac{R^{\frac{3n+1}{n}}}{2} - \frac{n}{3n+1}R^{\frac{3n+1}{n}}\right) \tag{6}$$

$$\frac{\partial p}{\partial x} = -2\mu\left[\frac{R^2(n+1)\overline{U}}{2n\left(\frac{R^{\frac{3n+1}{n}}}{2} - \frac{n}{3n+1}R^{\frac{3n+1}{n}}\right)}\right]^n \tag{7}$$

Figure 4 shows the velocity profile along the tube length by using power-law model.

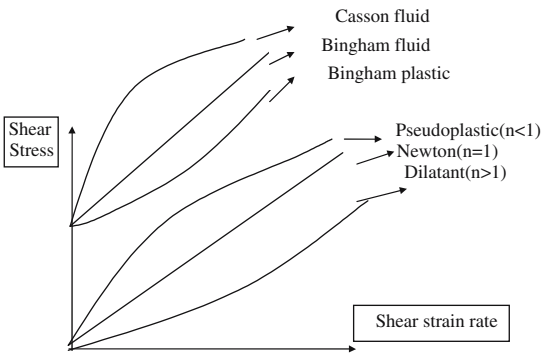

Fig. 2. Shear strain rate with respect to shear stress.

THE BINGHAM MODEL

The Bingham model is defined as:

$$\tau_{yx} = -\mu_0\frac{dV_x}{dy} \pm \tau_0; \quad \text{if}\left|\tau_{yx}\right|\tau_0$$

$$\frac{dV_x}{dy} = 0; \quad \text{if}\left|\tau_{yx}\right| < \tau_0 \tag{8}$$

The positive sign is used in above equation when τ is positive and the negative sign is used when τ is negative.

The Bingham model remains rigid when the shear stress is of smaller magnitude than the yield stress τ_0 but flows somewhat like a Newtonian fluid when the shear stress exceeds τ_0. This model has been found reasonably accurate for many fine suspensions and pastes. Bingham parameters for suspensions of nuclear fuel particles in heavy water are given [10] (Figure 3).

The velocity distribution using the model is obtained by the shell method as:

$$V_z = \frac{(P_0 - P_L)R^2}{4\mu_0 L}\left[1 - \left(\frac{r}{R}\right)^2\right] - \frac{\tau_0 R}{\mu_0}\left[1 - \left(\frac{r}{R}\right)\right];$$

when, $r \geq r_0 \quad r \leq r_0$

$$\text{For } V_z = \frac{(P_0 - P_L)R^2}{4\mu_0 L}\left[1 - \frac{r_0}{R}\right]^2 \tag{9}$$

The volume flow rate is calculated [15, 16]:

$$Q = V_z r\,dr d\theta = 2\pi\int_0^{r_0} V_Z^{<} r\,dr + 2\pi\int_{r_0}^{R} V_Z^{r}\,dr =$$

$$Q = \frac{\pi(P_0 - P_L)R^4}{8\mu_0 L}\left[1 - \frac{4}{3}\left(\frac{\tau_0}{\tau_R}\right) + \frac{1}{3}\left(\frac{\tau_0}{\tau_R}\right)^4\right] \tag{10}$$

And the pressure gradient is obtained by

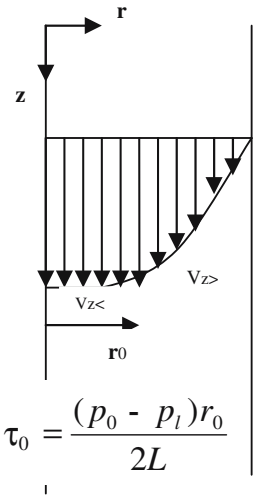

$$\tau_0 = \frac{(p_0 - p_l)r_0}{2L}$$

Fig. 3. Velocity profile along the tube.

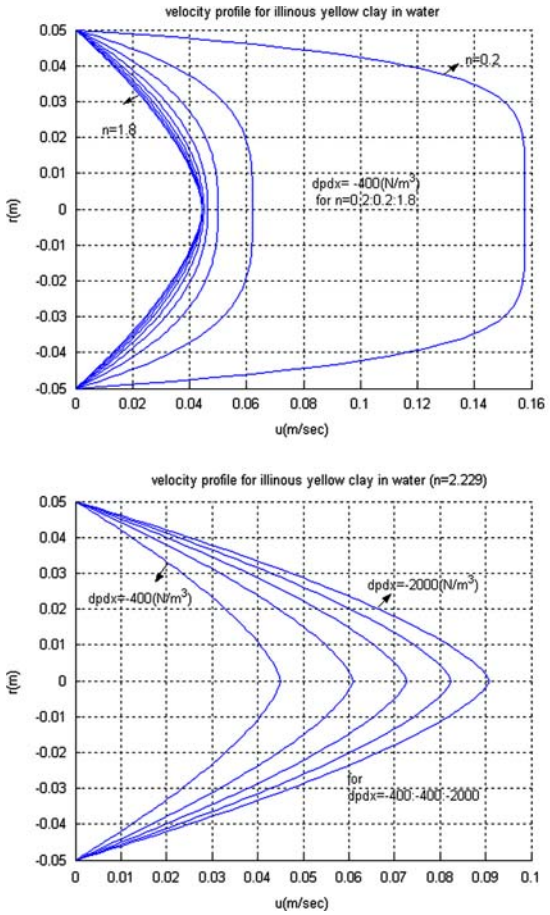

Fig. 4. Velocity profile with respect to the pipe radius for power law fluid, for the cases: constant and variable pressure gradient.

$$\left(-\frac{\partial P}{\partial x}\right)=\left[\frac{8\mu_0\overline{U}}{R^2\left[1-\frac{4}{3}\left(\frac{r_0}{R}\right)+\frac{1}{3}\left(\frac{r_0}{R}\right)^4\right]}\right] \tag{11}$$

Figure 5 shows velocity profile along the tube by using Bingham model.

THE CASSON MODEL

The Casson model is defined as:

$$\begin{aligned}\sqrt{\tau}&=\sqrt{\mu\dot{\gamma}}+\sqrt{\tau_0};\text{when}\quad \tau\geq\tau_0\\ \dot{\gamma}&=0;\text{when}\quad \tau<\tau_0\\ r_{\mathrm{p}}&=\frac{2\tau_0}{(-\partial P/\partial x)}\\ R_{\mathrm{p}}&=\frac{r_{\mathrm{p}}}{R}\end{aligned} \tag{12}$$

r_{p} plug radius:

With defining two above expressions and defining:

$$\begin{aligned}\dot{\gamma}&=-\frac{du}{dr}\\ \tau&=\frac{(-\partial p/\partial x)r}{2}\end{aligned} \tag{13}$$

If we substitute the two above expressions in equation (12) we can obtain velocity distribution (u).

Where in:

$$\begin{aligned}&r=r_{\mathrm{p}}\Rightarrow u=u_{\mathrm{p}}\\ &u=u_{\mathrm{p}}+\left(\frac{\partial P}{\partial x}\right)\frac{1}{4\mu}\left(r^2+2rr_{\mathrm{p}}-\frac{8}{3}\sqrt{r_{\mathrm{p}}r^3}-\frac{1}{3}r_{\mathrm{p}}^2\right)\\ &u_{\mathrm{p}}=\left(-\frac{\partial P}{\partial x}\right)\frac{1}{4\mu}\left(\sqrt{R}-\sqrt{r_{\mathrm{p}}}\right)^3\left(\sqrt{R}+\frac{1}{3}\sqrt{r_{\mathrm{p}}}\right)\end{aligned} \tag{14}$$

And the average velocity becomes:

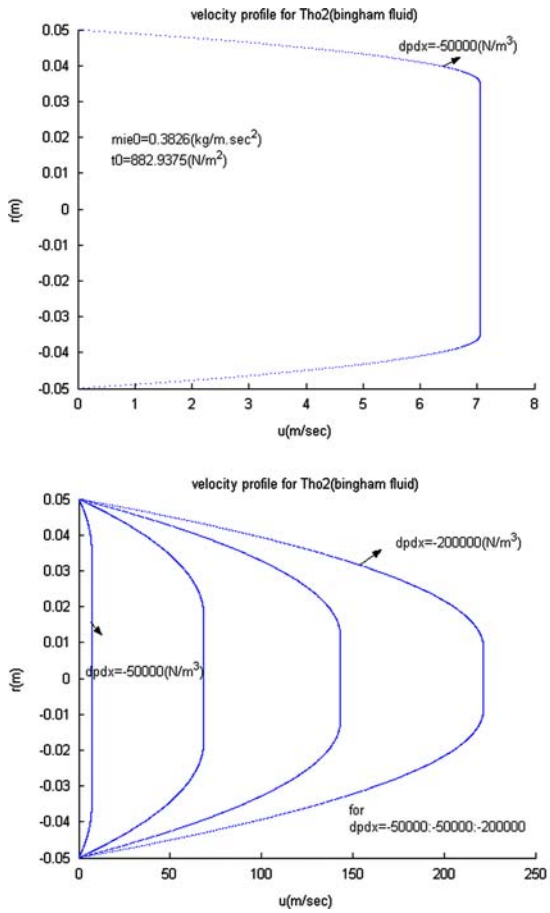

Fig. 5. Velocity profile with respect to the pipe radius for Bingham fluid, for the cases: constant and variable pressure gradient.

$$\overline{U} = \frac{R^2}{8\mu}\left(-\frac{\partial P}{\partial x}\right)\left(1 - \frac{16}{7}R_{\mathrm{p}}^{\frac{1}{2}} + \frac{4}{3}R_{\mathrm{p}} - \frac{1}{21}R_{\mathrm{p}}^4\right) \quad (15)$$

Figure 6 shows velocity profile along the tube by using Casson model.

TOTAL ENTROPY GENERATION FOR LAMINAR VISCOUS NON-NEWTONIAN FLOW THROUGH A PIPE

The entropy generation within the control volume in Figure 1 can be written as:

$$\dot{ds}_{\mathrm{gen}} = \dot{m}\, ds - \frac{\delta \dot{Q}}{T_{\mathrm{w}}}$$

Where for an incompressible fluid,

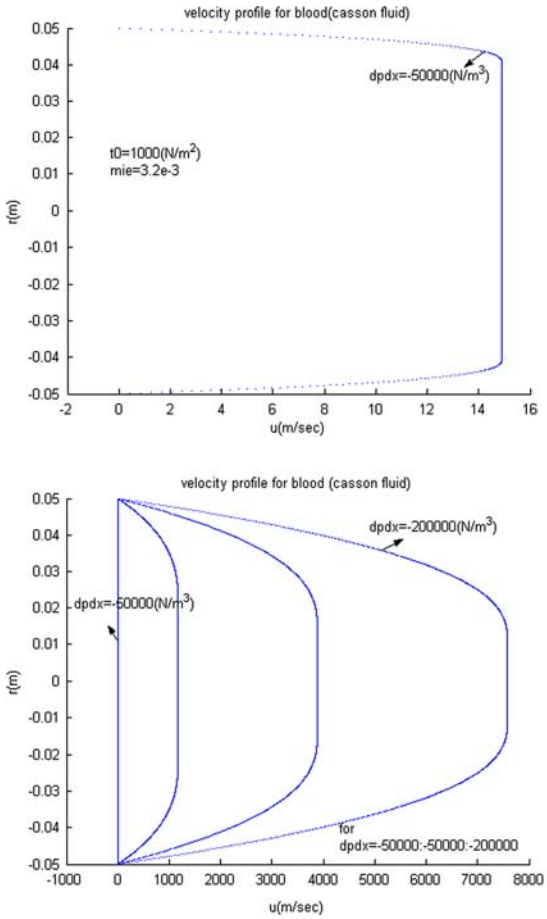

Fig. 6. Velocity profile with respect to the pipe radius for Casson fluid, for the cases: constant and variable pressure gradient.

$$ds = \frac{C_p dT}{T} - \frac{dP}{\rho T} \quad (16)$$

By substituting in the above equations, the total entropy generation becomes,

$$d\dot{S}_{\mathrm{gen}} = \dot{m}\, C_p\left(\frac{T_{\mathrm{w}} - T}{T T_{\mathrm{w}}}dT - \frac{1}{\rho C_p T}dP\right) \quad (17)$$

Using power-law fluid with constant viscosity the following relation is obtained for entropy generation:

$$\dot{S_{\mathrm{gen}}} = \dot{m}\, C_p\left\{\ln\left(\frac{1-\tau e^{-4}\prod_1}{1-\tau}\right) - \tau\left(1 - e^{-4}\prod{}^1\right) + \frac{2\tau\prod_2 R^2}{\bar{U}}\left(\frac{R^2(n+1)\overline{U}}{2n\left(\frac{R^{\frac{3n+1}{n}}}{2} - \frac{n}{3n+1}R^{\frac{3n+1}{n}}\right)}\right)^n \ln\left(\frac{e^4\prod_1 - \tau}{1-\tau}\right)\right\} \quad (18)$$

For Bingham fluid, the entropy generation is reached by

$$\dot{S_{\mathrm{gen}}} = \dot{m}\, C_p\left\{\ln\left(\frac{1-\tau e^{-4}\prod_1}{1-\tau}\right) - \tau\left(1 - e^{-4}\prod{}^1\right) + \frac{8\tau\prod_2}{\left[1 - \frac{4}{3}\left(\frac{r_0}{R}\right) + \frac{1}{3}\left(\frac{r_0}{R}\right)^4\right]}\ln\left(\frac{e^4\prod_1 - \tau}{1-\tau}\right)\right\} \quad (19)$$

For Casson fluid, the entropy generation is achieved by

$$\dot{S_{\mathrm{gen}}} = \dot{m}\, C_p\left\{\ln\left(\frac{1-\tau e^{-4}\prod_1}{1-\tau}\right) - \tau\left(1 - e^{-4}\prod{}^1\right) + \frac{8\tau\prod_2}{\left[1 - \frac{16}{7}\left(\frac{r_{\mathrm{p}}}{R}\right)^{0.5} + \frac{4}{3}\left(\frac{r_{\mathrm{p}}}{R}\right) - \frac{1}{21}\left(\frac{r_{\mathrm{p}}}{R}\right)^4\right]}\ln\left(\frac{e^4\prod_1 - \tau}{1-\tau}\right)\right\} \quad (20)$$

where τ is the dimensionless temperature difference,

$$\tau = \frac{T_{\mathrm{w}} - T_0}{T_{\mathrm{w}}} \quad (21)$$

and Ec is the Eckert number defined as:

$$Ec = \frac{\bar{U}^2}{C_p(T_{\mathrm{w}} - T_0)} \quad (22)$$

Two dimensionless groups in fully developed laminar flow are as

$$\prod_1 = St\frac{l}{D} \tag{23}$$

and

$$\prod_2 = \frac{Ec}{St\,Re} \tag{24}$$

Now, defining dimensionless entropy generation as [17]:

$$\psi = \frac{\dot{S}_{\text{gen}}}{(\dot{Q}/T_w - T_0)}$$

equation (16) can be written as:

$$\psi = \frac{1}{1-e^{-4\prod_1}}\left\{\ln\left(\frac{1-\tau e^{-4\prod_1}}{1-\tau}\right) - \tau\left(1-e^{-4\prod 1}\right) + \frac{2\tau\prod_2 R^2}{\bar{U}}\left(\frac{R^2(n+1)\overline{U}}{2n\left(\frac{R^{\frac{3n+1}{n}}}{2} - \frac{n}{3n+1}R^{\frac{3n+1}{n}}\right)}\right)^n \ln\left(\frac{e^4\prod_1 - \tau}{1-\tau}\right)\right\} \tag{25}$$

Also, the dimensionless entropy generation for the Bingham model is obtained as:

$$\psi = \frac{1}{1-e^{-4\prod_1}}\left\{\ln\left(\frac{1-\tau e^{-4\prod_1}}{1-\tau}\right) - \tau\left(1-e^{-4\prod 1}\right) + \frac{8\tau\prod_2}{\left[1-\frac{4}{3}\left(\frac{r_0}{R}\right)+\frac{1}{3}\left(\frac{r_0}{R}\right)^4\right]}\ln\left(\frac{e^4\prod_1 - \tau}{1-\tau}\right)\right\} \tag{26}$$

and for Casson model:

$$\psi = \frac{1}{1-e^{-4\prod_1}}\left\{\ln\left(\frac{1-\tau e^{-4\prod_1}}{1-\tau}\right) - \tau\left(1-e^{-4\prod 1}\right) + \frac{8\tau\prod_2}{\left[1-\frac{16}{7}\left(\frac{r_p}{R}\right)^{0.5}+\frac{4}{3}\left(\frac{r_p}{R}\right)-\frac{1}{21}\left(\frac{r_p}{R}\right)^4\right]}\ln\left(\frac{e^4\prod_1 - \tau}{1-\tau}\right)\right\} \tag{27}$$

PUMPING POWER TO HEAT TRANSFER RATE RATIO

The ratio of the pumping power to heat transfer rate is [17]:

$$P_r = \frac{\left(\frac{\pi}{4}D^2\right)(\Delta p)\,\bar{U}}{\dot{Q}}$$

Using pressure gradient for three models, pumping power to heat transfer rate ratio is obtained, for power-law model as:

$$P_r = \left(\frac{8R^2}{\overline{U}}\right)\left(\frac{R^2(n+1)\overline{U}}{2n(\frac{R^{\frac{3n+1}{n}}}{2} - \frac{n}{3n+1}R^{\frac{3n+1}{n}})}\right)^n \frac{\prod_1\prod_2}{1-e^{-4\prod_1}} \tag{28}$$

Also for Bingham model as:

$$P_r = \left(\frac{1}{1-\frac{4}{3}\left(\frac{r_0}{R}\right)+\frac{1}{3}\left(\frac{r_0}{R}\right)^4}\right)\frac{32\prod_1\prod_2}{\left(1-e^{-4\prod_1}\right)} \tag{29}$$

and for Casson model:

$$P_r = \left(\frac{1}{1-\frac{16}{7}\left(\frac{r_p}{R}\right)^{0.5}+\frac{4}{3}\left(\frac{r_p}{R}\right)-\frac{1}{21}\left(\frac{r_p}{R}\right)^4}\right)\frac{32\prod_1\prod_2}{\left(1-e^{-4\prod_1}\right)} \tag{30}$$

DISCUSSIONS

In this paper, we used three kinds of non-Newtonian fluids and the thermo physical properties used in the numerical example are given in Table 1. The surface temperature, the velocity of the incompressible fluid, and the cross-sectional area of the pipe were fixed. The length of the pipe and the inlet fluid temperature are the variables.

Figures 4–6 show the velocity profiles with respect to the pipe radius for three kinds of non-Newtonian fluids. We observe that by decreasing n and also by increasing the pressure gradient, the velocity profiles moving to the right direction and the center line velocity increases significantly.

Figure 7 shows the variation of dimensionless entropy generation, ψ, with respect to modified Stanton number, for three models. Since $\prod_1$ represents the length of the pipe, the dimensionless entropy generation defined on the basis of total heat transfer rate to the pipe decreases along the pipe length. The rate of increase in entropy generation decreases and approaches a constant value as the total heat transfer rate to the fluid approaches its maximum value of

Table 1. Thermophysical Properties and Parameters

Casson model (kg/m s)	Bingham model	Power-law model	μ
3.2×10^{-3}	(kg/m s) 0.3826	(kg/m $s^{2.229}$) 5.5041	
–	–	2.229	n
1000	882.9375	–	Shear stress (N/m^2)
373	373	373	($'k$) T_w
293	293	293	($'k$)T_0
0.5–0	0.5–0	0.5–0	$\prod_1$
0.1	0.1	0.1	D (m)
18.3	14.64	47.58	$\bar{h}\left(\frac{w}{m^2 \cdot k}\right)$

Figure 8 shows the effect of the $\dot{Q}_{max} = \dot{m}C_p(T_w - T_0)$ pressure gradient on the dimensionless entropy generation, we observed that when the pressure gradient increases, the values of average velocity and $\prod_2$ increases, on the other hand, the last term in equations (25–27) would be increased, consequently the amount of ψ would be increased.

Figure 9 shows the variation of the dimensionless entropy generation, ψ, with respect to the dimensionless inlet wall-to-fluid temperature difference, τ, for three models. Since τ represents the difference between the temperature of the pipe surface and that of the inlet fluid, the dimensionless entropy generation defined due to the increase in the total heat transfer rate to the fluid. For small values of τ, the total entropy change is due to the viscous friction and noting that the product ($\tau \prod_2$) is independent of the inlet fluid temperature.

Figure 10 shows the pumping power to heat transfer rate ratio with modified Stanton number ($\prod_1$). It appears that by increasing $\prod_1$, it yields unreasonably high pumping power ratio as expected. For large values of $\prod_1$, it can be shown from equations (28–30), that the pumping ratio, P_r, increases linearly with the slope of the profile.

The slope for power-law becomes:

$$\frac{dP_r}{d\prod_1} = \left(\frac{8R^2 \prod_2}{\overline{U}}\right)\left(\frac{R^2(n+1)\overline{U}}{2n(\frac{R^{\frac{3n+1}{n}}}{2} - \frac{n}{3n+1}R^{\frac{3n+1}{n}})}\right)^n \quad (31)$$

Also, for Bingham model as:

$$\frac{dP_r}{d\prod_1} = \left(\frac{32\prod_2}{1 - \frac{4}{3}\left(\frac{r_0}{R}\right) + \frac{1}{3}\left(\frac{r_0}{R}\right)^4}\right) \quad (32)$$

Also for Casson model as:

$$\frac{dP_r}{d\prod_1} = \left(\frac{32\prod_2}{1 - \frac{16}{7}\left(\frac{r_p}{R}\right)^{0.5} + \frac{4}{3}\left(\frac{r_p}{R}\right) - \frac{1}{21}\left(\frac{r_p}{R}\right)^4}\right) \quad (33)$$

Figure 11 shows the pumping power to heat transfer rate ratio, P_r, with respect to the dimensionless inlet wall-to-fluid temperature difference, τ for three models, we observe that, the product ($\tau \prod_2$) is invariable with varying inlet fluid temperature, it can be concluded from equations (28–30) that the pumping power ratio is inversely proportional to τ.

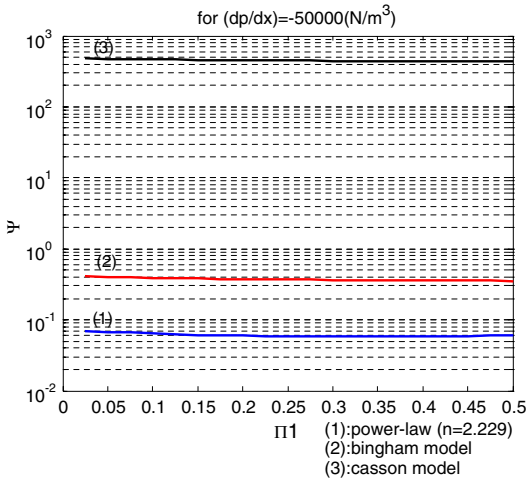

Fig. 7. The variation of the dimensionless entropy generation with respect to modified Stanton Number for 3 case of non-Newton fluids, for $(dp/dx) = -50000$ (N/m^3).

CONCLUSIONS

In this paper the velocity profile with respect to the pipe radius for three non-Newtonian models i.e. power-law, Bingham model and Casson model has been investigated. The entropy generation using the model with constant viscosity is calculated and it is observed that by increasing modified Stanton number ($\prod_1$) and dimensionless inlet wall-to-fluid temperature difference (τ), the entropy generation increases significantly. Also, it was found that, the pumping

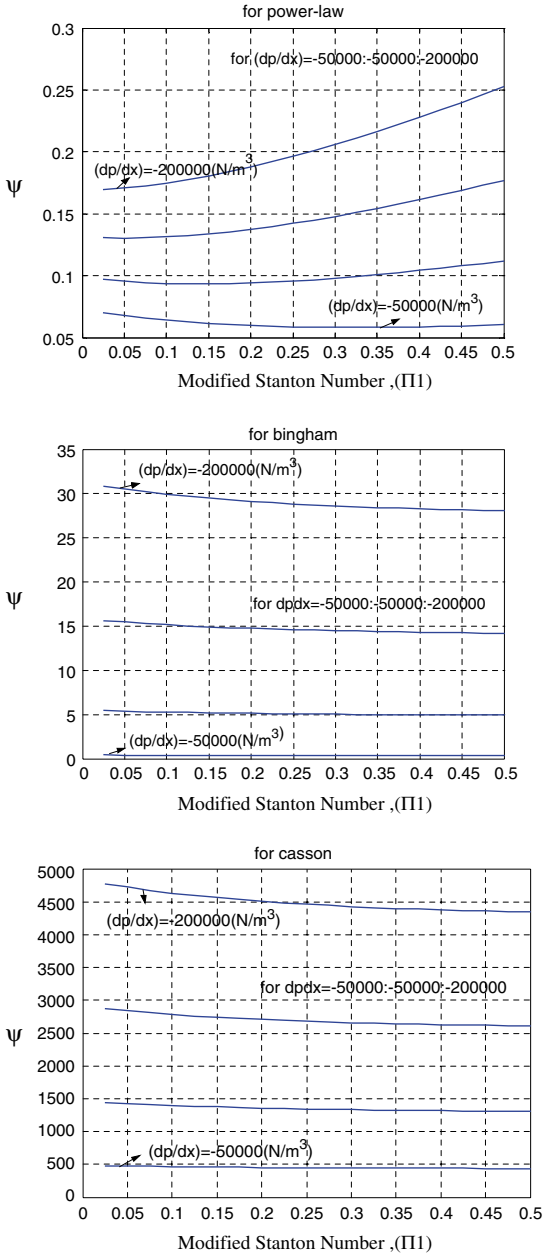

Fig. 8. The variation of the dimensionless entropy generation with respect to modified Stanton Number for three models, for different pressure gradient.

power to heat transfer rate ratio (P_r) decreases by increasing dimensionless inlet wall-to-fluid temperature difference. It was found that in any three models when the value $\prod_1$ is small, ψ decreases when $\prod_1$ increases. As value $\prod_1$ is becoming bigger, the value ψ is increased. It should be noticed that when the value $\prod_1$ has become very big , P_r increases significantly.

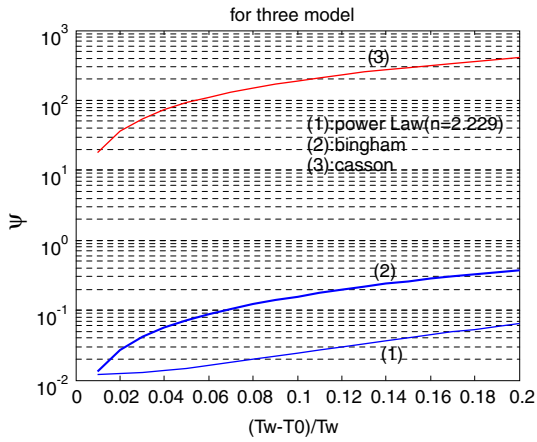

Fig. 9. The variation of the dimensionless entropy generation with respect to dimensionless inlet wall-to-fluid temperature difference, τ, for three models.(dp/dx) = −50000 (N/m^3).

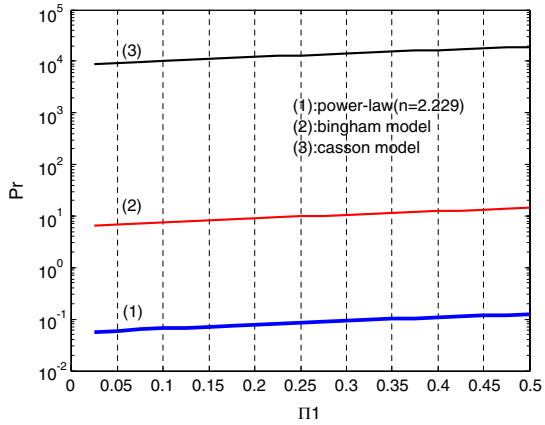

Fig. 10. The variation of the pumping power to heat transfer rate ratio with respect to modified Stanton Number, $\prod 1$, for three models. (dp/dx) = −50000 (N/m^3).

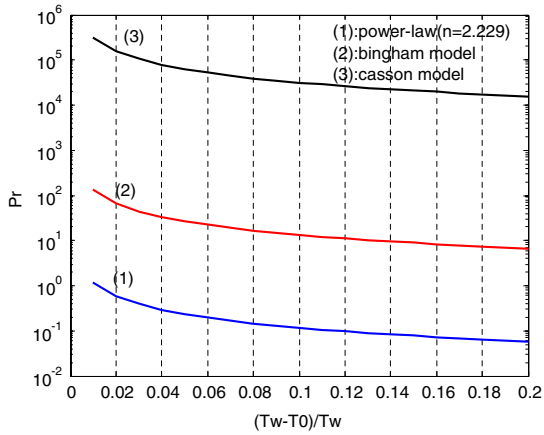

Fig. 11. The variation of the pumping power to heat transfer rate ratio with respect to dimensionless inlet wall-to-fluid temperature difference, τ, for three models. (dp/dx) = −50000 (N/m^3).

REFERENCES

1. A. Bejan, *ASME, J. Heat Transfer*, **101**, 718–725 (1979)
2. A. Bejan, *Energy*, **5**, 721–732 (1980)
3. A. Bejan, *Adv. Heat Transfer*, **15**, 1–58 (1982)
4. A. Bejan, *Advanced Engineering Thermodynamics* (John Wiley & Sons Inc., New York, 1988), pp. 594–602
5. C. G. Carrington, and Z. F. Sun, *Int. J. Heat Fluid Flow*, **13**, 65–70 (1992)
6. A. S. Gbadebo, B. S. Yilbas, and K. Boron, *Int. J. Energy Res.*, **23**, 1101–1110 (1999)
7. W. M. Kays, and A. L. London, *Compact Heat Exchangers* (Mc Graw-Hill, New-York, 1958), pp. 49
8. M. Knudsen, *the Kinetic Theory of Gases* (Methuen, London, 1934)
9. E. H. Kennard, *Kinetic Theory of Gases* (Mc Graw-Hill, New-York, 1938)
10. J. A. Lane, MacPherson and F. Masalan, *Transport phenomena* (Addison-Wesley, Reading, Mass., 1958), Contributed by Thomas, D.G
11. H. G. Langeroudi and C. Aghanajafi, Int. J. Fusion Energy, **25**, (this issue) (2006)
12. A. B. Metzner, *Advanced in Chemical Engineering* I (Academic Press, New York, 1956), pp. 103
13. G. N. Patterson, *Molecular Flow of Gases* (Wiley, New York, 1956)
14. J. H. Perry, *Chemical Engineers Hand Book*, *3rd ed.* (Mc Graw-Hill, New York, 1950), pp. 388–389
15. M. Reiner, In F. R. Eirich (Ed.), Phenomenological Macro-rheology, Chapter 2 in Rheology, Vol. 1 (Academic Press, New York, 1956), p. 45
16. M. Reiner, *Deformation, Strain, and flow* (Interscience, New York, 1960)
17. A. Z. Sahin, *Int. J. Heat Mass Transfer*, **120**, 76–83 (1998)ASME